Lobate Scarp Modeling with Lunar Reconnaissance Orbiter Camera Digital Terrain Models

Nathan R. Williams[1], Thomas R. Watters[2], Matthew E. Pritchard[3], Maria E. Banks[2], James F. Bell III[1], Mark S. Robinson[1], Thanh Tran[1]

[1]Arizona State University; [2]NASM/Smithsonian Institution; [3]Cornell University; (nrwilli2@asu.edu)

P43D
1707

Introduction to Lobate Scarps

- Linear or curvilinear hills with steep face and gently sloping back[1-3]
- Interpreted as surface expressions of shallow thrust faults
- Distributed globally across Moon
- Thought to form by global thermal radial contraction
- Typically tens of meters high and tens to hundreds of kilometers long

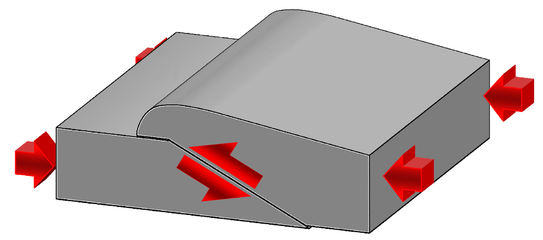

Fig. 1: Illustrated block diagram of a scarp

Motivation

- Subsurface geometries of faults, depth ranges, offsets, mechanical properties and stratification in the lithosphere are poorly understood for lunar lobate scarps[1,4,5,6]
- Radial contraction of the Moon can be inferred from the contraction across lobate scarps globally[1-3]
- High-resolution observations provide valuable insight into lunar surface and subsurface processes

Data and Methods

- Lunar Reconnaissance Orbiter Camera (LROC) has two 50 cm/px Narrow Angle Cameras (NACs) & a ~100 m/px Wide Angle Camera (WAC)[7]
- High-resolution 2 m/post digital terrain models (DTMs) from stereo NAC pairs and Lunar Orbiter Laser Altimeter (LOLA) ranging tracks[8,9] and 100 m/post WAC DTMs for context[10]
- COULOMB models surface deformation for fault dislocations in an elastic half-space[11-13]
- Displacement, dip, depth, and taper varied to fit fault model to detrended DTM profile

Slipher Scarp

- 48.3º N, 160.6º E
- Verges upslope on slump bench of Slipher crater wall
- Continues eastward along rim of D'Alembert crater
- Splays into several sub-parallel segments
- Fault dislocation model with five 75 m fault taper steps suggests 40º slope from surface to 200 m depth

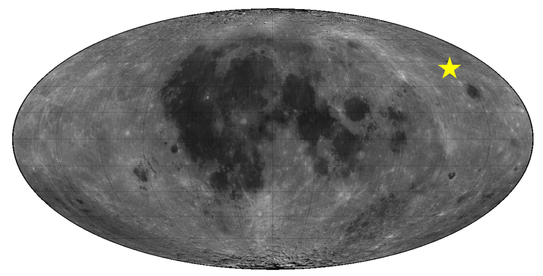

Fig. 2: Location of Slipher scarp

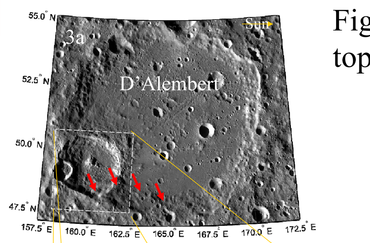

Fig. 3a-d: LROC WAC regional image mosaic and topography of D'Alembert and Slipher craters

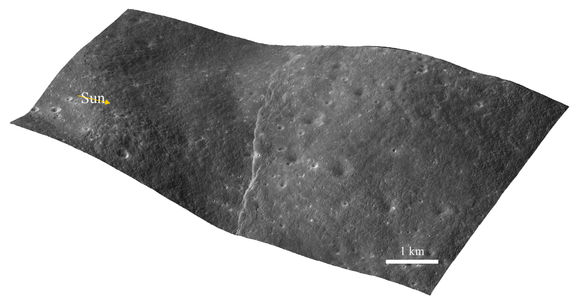

Fig. 4: LROC NAC DTM of Slipher scarp

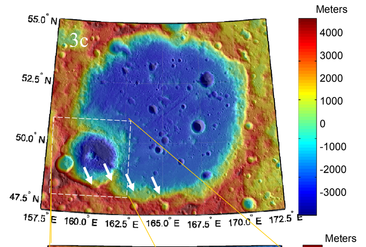

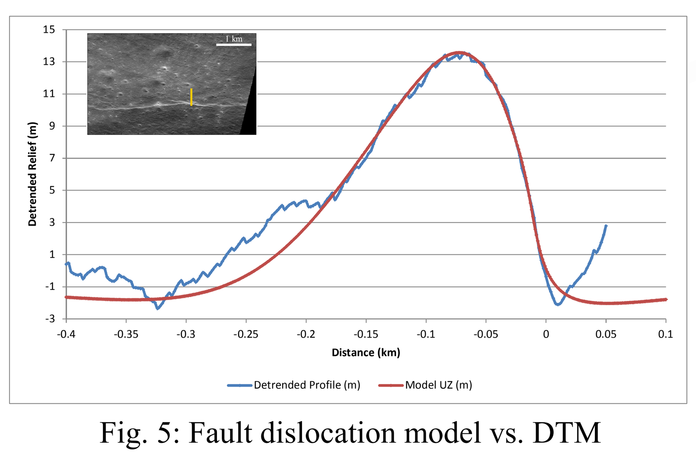

Fig. 5: Fault dislocation model vs. DTM topographic profile at inset location (orange)

Simpelius S-1 Scarp

- 73.5º S, 13.1º E
- Multiple segments along crater rim and continuing southwest
- Changes vergence along strike
- Fault dislocation model with five 50 m fault taper steps suggests 35º slope from surface to 220 m depth

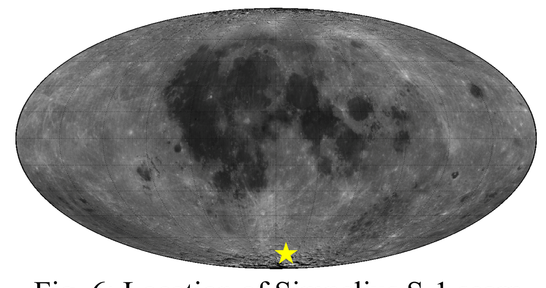

Fig. 6: Location of Simpelius S-1 scarp

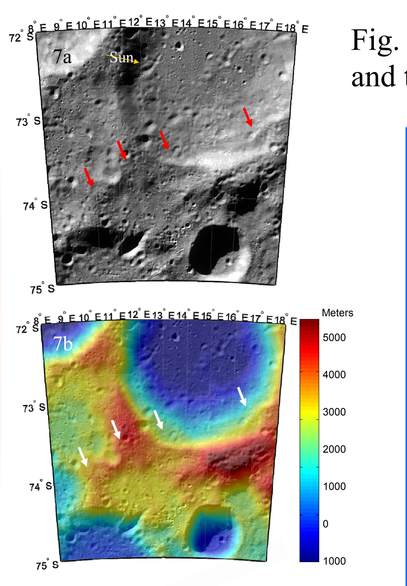

Fig. 7a-b: LROC WAC regional image mosaic and topography around Simpelius S-1 scarp

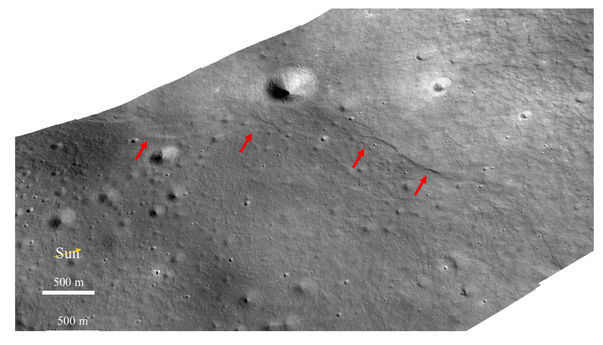

Fig. 8: LROC NAC DTM of Simpelius S-1 scarp

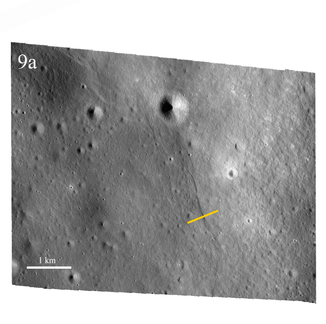

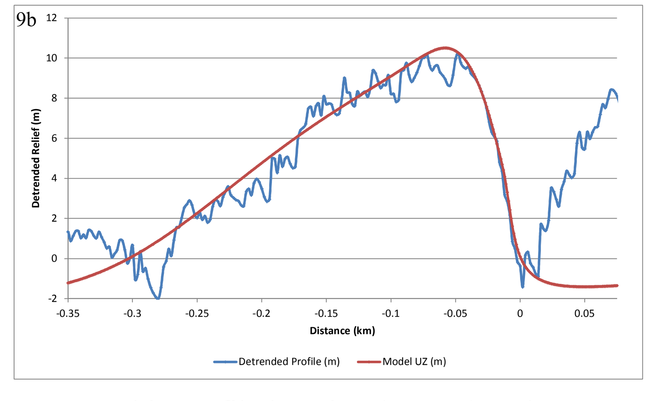

Fig. 9: a) DTM topographic profile location (orange) and b) comparison between DTM profile and fault dislocation model

Racah X-1 Scarp

- 10.1º S, 178.1º E
- Single large scarp running N-S in hummocky terrain
- Fault dislocation model with five 250 m fault taper steps suggests 38º slope from surface to 900 m depth

Fig. 10: Location of Racah X-1 scarp

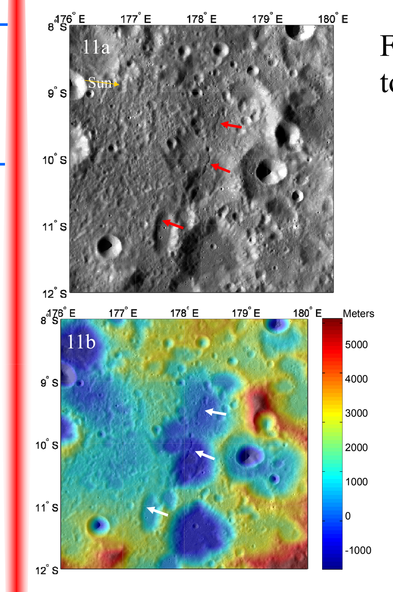

Fig. 11a-b: LROC WAC regional image mosaic and topography around Racah X-1 scarp

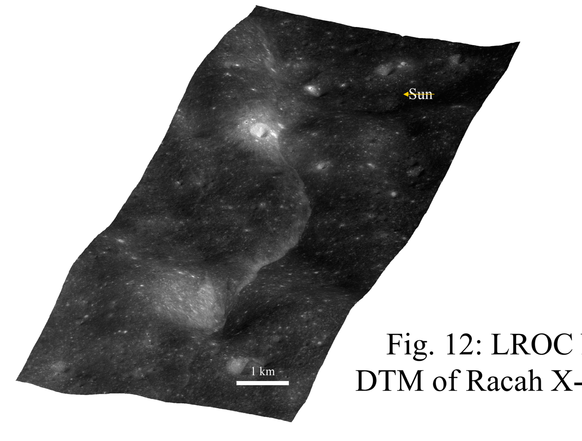

Fig. 12: LROC NAC DTM of Racah X-1 scarp

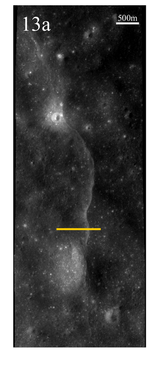

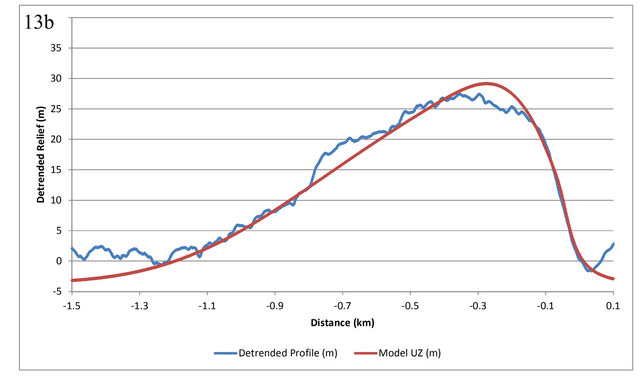

Fig. 13: a) DTM topographic profile location (orange) and b) comparison between profile and fault dislocation model

Summary

- LROC NAC DTMs enable quantitative measurements of scarp morphology at high resolutions
- Fault dislocation models for surface-breaking thrust faults match observed topography
- Models show lobate scarp faults have shallow dips 35º-40º
- Faults occur from surface to depths of several hundred meters
- Comparable to Hinks Dorsum on asteroid 433 Eros (~35º dip, maximum depth 240 m)[14]
- Order of magnitude smaller than scarps on Mercury and Mars (up to 1 km in relief)[15,16]

Future Work

- Make and compare fault dislocation models of other scarps globally as more DTMs become available
- Add regolith creep / diffusion to models
- Re-calculate displacements and global contraction with future catalog of revised dip and depth estimates
- Create and compare fault dislocation models for lunar wrinkle ridges, esp. near ridge-scarp transitions

References

[1] Watters T.R. and Johnson C.L. (2010) in *Planetary Tectonics*, Cambridge Univ. Press, 121-182. [2] Watters T.R. et al. (2010) *Science, 329*, 936-940. [3] Binder A.B. and Gunga H.C. (1985) *Icarus, 63*, 421-441. [4] Watters T.R. (2004) *Icarus*, 171, 284-294. [5] Schultz R.A. (2000) JGR, 105, 12,035-12,052. [6] Mueller K. and Golombek M. (2004) *Annu. Rev. Earth Planet. Sci.*, 435-464. [7] Robinson M.S. et al. (2010) *Space Sci. Rev.*, *150*, 81-124. [8] Smith D.E. et al. (2010) *Space Sci. Rev.*, 150, 209. [9] Tran T. et al. (2010) ISPRS, #7161. [10] Scholten F. et al. (2011) *Proc. of Lun. & Plan Sci. Conf.*, 42, 2046. [11] Okada Y. (1992) *Bull. Seismol. Soc. Am.*, 82, 1018–1040. [12] Toda S. et al. (2005) *JGR*, 110, B05S16. [13] Lin J. (2004) *JGR*, 109, B02303. [14] Watters T.R. et al. (2011) *Geophys. Res. Let.*, 38, L02202. [15] Watters T.R. et al (2009) *Earth & Plan. Sci. Let.*, 285, 283-296. [16] Watters T.R. and Robinson M.S. (1999) *JGR*, 104, 18,981-18,990.